Tuning the nuclearity of [Mo2O2S2]2+ -based assemblies by playing with the degree of flexibility of bis-thiosemicarbazone ligands

Diana Cebotari, Sergiu Calancea, Jerôme Marrot, Régis Guillot, Clément Falaise, Vincent Guérineau, David Touboul, Mohamed Haouas, Aurelian Gulea, Sébastien Floquet

ARTICLE

Tuning the nuclearity of $[Mo_2O_2S_2]^{2+}$-based assemblies by playing with the degree of flexibility of bis-thiosemicarbazone ligands

Received 00th January 20xx,
Accepted 00th January 20xx

DOI: 10.1039/x0xx00000x

Diana Cebotari,[a,b] Sergiu Calancea,[a] Jerôme Marrot,[a] Régis Guillot,[c] Clément Falaise,[a] Vincent Guérineau,[d] David Touboul,[d] Mohamed Haouas,[a] Aurelian Gulea,*[b] and Sébastien Floquet*[a]

The $[Mo^{V}_2O_2S_2]^{2+}$-based thiosemicarbazone complexes appear as very promising molecules for biological applications due to the intrinsic properties of their components. This paper deals with the synthesis and the characterization of six coordination complexes obtained by reaction of $[Mo^{V}_2O_2S_2]^{2+}$ cluster with bis-thiosemicarbazone ligands that contain flexible or rigid spacers between the two thiosemicarbazone units. Interestingly, the structural characterizations by single-crystal X-ray diffraction, MALDI-TOF MS technique and NMR spectroscopy, revealed that the nuclearity of complex is controlled by the nature of the spacer between the thiosemicarbazone units. Binuclear complexes, namely $[Mo^{V}_2O_2S_2(L^{1\text{-}3})]$, are isolated with flexible spacers while tetranuclear complexes $[(Mo^{V}_2O_2S_2)_2(L^{4\text{-}6})_2]$ are formed when the bis-thiosemicarbazone ligands is built on rigid spacer.

Introduction

Molybdenum (Mo) is an essential trace element found in more than fifty molybdoenzymes. In these enzymes, the molybdenum atoms, mainly found as Mo^{VI} or Mo^{V}, are usually surrounded by oxygen, nitrogen and sulfur atoms, and these active centers are known for catalysing different transfer reactions in the metabolism of bacteria, plants and animals.[1-3] Driven by these biological features, the coordination chemistry of dimolybdic clusters $[Mo^{V}_2O_4]^{2+}$ and $[Mo^{V}_2O_2S_2]^{2+}$ has been historically studied to design biomimetic models[4,5] of molybdoenzymes. Later, the dimolybdic clusters have been widely employed as building blocks for supramolecular chemistry with polyoxometalates.[6] More recently, such Mo^{V} containing entities have been identified as efficient catalysts for hydrogen evolution reaction.[7]

Surprisingly, despite number of $[Mo^{V}_2O_2S_2]^{2+}$-based complexes having similar coordination sphere as molybdoenzymes, only few biological studies were reported until recently. Indeed, Suman's group, using different S, O and N-based organic ligands, has reported $[Mo^{V}_2O_2S_2]^{2+}$ complexes can act as low cytotoxicity catalytic drugs, notably for treatment against cyanide poisoning.[8-11] Besides, exploring the coordination chemistry of dimolybdic clusters with L-amino acids and various amino carboxylic acids, our group observed relevant structure dependent antioxidant activity.[12] Therefore, the combination of $[Mo^{V}_2O_2S_2]^{2+}$ cluster with bioactive ligands represents an appealing strategy to develop new classes of coordination complexes with emerging biological properties arising from intrinsic properties of each component. In this case, the thiosemicarbazone ligands (Scheme 1) are very interesting candidates, notably due their O,N,S donating atoms similar to the coordination sphere of natural enzymes.

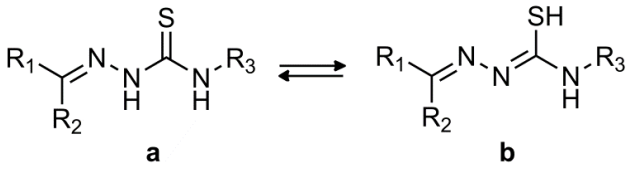

a b

Scheme 1 Tautomeric forms of thiosemicarbazone ligands

The nature of substituents R_1, R_2, R_3 can be easily tuned, thus giving thousands of ligands and transition metal complexes, well-known to exhibit important antitumor, antiviral, antibacterial, antifungal, and antimalarial activities.[13-29] The Mo-thiosemicarbazone complexes described in the literature are often based on Mo^{VI}-dioxo moieties and exhibit antioxidant,[30] antitumor[31] and antibacterial[32] properties as well as catalytic properties.[33] In contrast, Mo^{V}-based thiosemicarbazones complexes are much scarce. Therefore, we recently started to explore the reactivity of the $[Mo^{V}_2O_2S_2]^{2+}$ cluster with a wide panel of thiosemicarbazone ligands. 14 complexes with stoichiometry cluster : ligand = 1 : 2 have been isolated by our group.[34] However, NMR studies have revealed

[a] Institut Lavoisier de Versailles, CNRS, UVSQ, Université Paris-Saclay, 45 av. des Etats-Unis, 78035 Versailles, France
[b] State University of Moldova, MD-2009 Chisinau, Republic of Moldova
[c] Institut de Chimie Moléculaire et des Matériaux d'Orsay, ICMMO, CNRS UMR 8182, Université Paris Saclay, 91405 Orsay Cedex, France
[d] Institut de Chimie des Substances Naturelles, CNRS UPR2301, Université Paris-Sud, Université Paris-Saclay, 91198 Gif-sur-Yvette Cedex, France
* Correspondence email: sebastien.floquet@uvsq.fr

† Electronic Supplementary Information (ESI) available: MALDI-TOF spectra (Figures S1-S5); views of crystal packing (Figures S6-S15); NMR spectra (^{1}H, ^{1}H DOSY, and ^{15}N{^{1}H} HMBC NMR) of ligands and complexes not given in the main text (Figures S16-S30). See DOI: 10.1039/x0xx00000x

in most cases the formation of isomeric mixtures, which is a serious drawback for the biological studies.

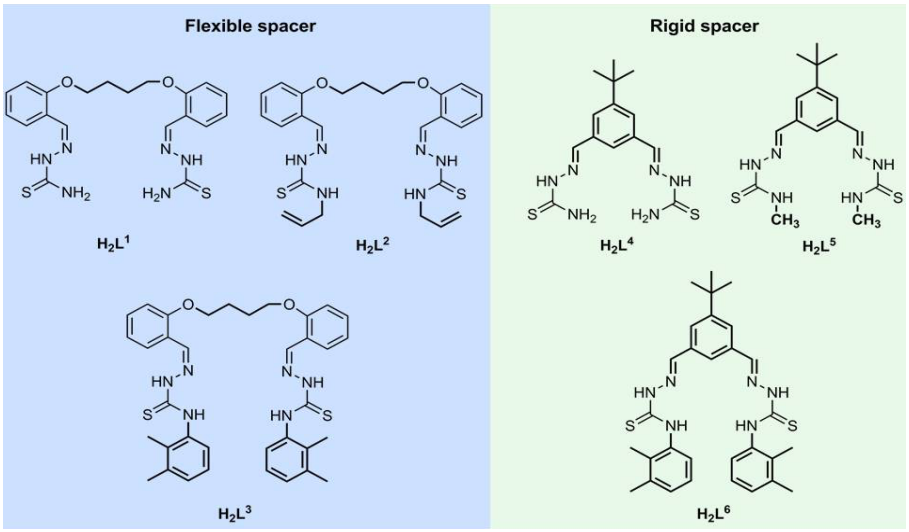

Scheme 2. The structures of bis-thiosemicarbazone ligands with flexible and rigid spacers

Some coordination features from the previous work can be drawn: i) when R_2 = H, two isomers *cis* and *trans* are obtained, ii) while for R_2 = Me, up to 8 isomers can be observed in solution, iii) in the case of R_1 fragments derived from aldehydes, no coordination with the $[Mo^{V}_2O_2S_2]^{2+}$ cluster can occur, contrary to what usually happens with 3d metal ions, and finally, iv) R_3 group appears to have no influence on the coordination of the ligand.

It is important to develop efficient molecular engineering approach to avoid the coexistence of several $[Mo^{V}_2O_2S_2]^{2+}$-based thiosemicarbazone isomers. We hypothesized that the use of bis-thiosemicarbazone ligands, that can act as bis(bidentate) ligand for the molybdic cluster, must favour the formation of only one molecular entity. In this work, six new bis-thiosemicarbazone ligands with flexible (H_2L^1-H_2L^3) or rigid (H_2L^4-H_2L^6) spacers have been synthesized (Scheme 2). The formation of complexes with $[Mo^{V}_2O_2S_2]^{2+}$ cluster were then investigated and the resulting products have been characterised both in the solid-state by single-crystal X-ray diffraction and in solution by ^{1}H, 2D ^{1}H{^{15}N} HMBC et ^{1}H DOSY NMR experiments. This set of results demonstrate the influence of the ligand design, especially the role of the spacer between the two thiosemicarbazone units, on the molecular topologies of $[Mo^{V}_2O_2S_2]^{2+}$ coordination complexes.

Experimental Section

Materials and methods

All chemicals were analytical grade and used without any further purification. IR spectra were recorded on a 6700 Fourier Transform Nicolet spectrophotometer, using diamond ATR technique in the range 400-4000 cm^{-1}. The elemental analysis for C, H, N and S were performed by Biocis company at Chatenay-Malabry, France.

MALDI-TOF MS analyses

The spectra were performed on UltrafleXtreme mass spectrometer (Bruker Daltonics, Bremen) calibrated with PEG1500 and PEG4500 polymers. All spectra were collected on powder samples in linear positive ion mode. All data were processed using Bruker Daltonics FlexAnalysis program and as the matrix was used Dithranol purchased from Sigma Aldrich Co. All samples were prepared as 60 µM THF-DMSO solutions using 6 mM matrix solution with or without addition of a sodium salt. The samples were prepared by adding the sample solution to matrix solution in a volume ratio of 1:9. The powders obtained after drying were analyzed by MALDI-TOF technique. The Simulations of spectra were performed with IsoPro 3.1. IsoPro is available as freeware from https://sites.google.com/site/isoproms/home.

Nuclear magnetic resonance

^{1}H, ^{1}H{^{15}N} HMBC et ^{1}H DOSY spectra were measured at 298 K on Bruker Avance 400 MHz spectrometer with 5 mm BBI probe head at 9.4 T. ^{13}C NMR was recorded with a Bruker Avance 300 MHz spectrometer. All samples were solubilised in DMSO-d_6 deuterated solvent. The ^{1}H spectra were recorded as standard procedure using one pulse sequence at 30° flip angle applying 2.8 µs duration pulse time, 2 s recycle delay, 1.6 s for acquisition time, and 8 number of scans. The 2D ^{1}H{^{15}N} HMBC spectra were recorded using standard Bruker pulse sequences with shortened recycle period to 1 s. The 50 ms mixing time corresponding to 1/2JH-N (JH-N = 10 Hz) was employed for ^{1}H{^{15}N} HMBC experiments. Translational diffusion measurements were performed by Bruker's "ledbpgs2s" stimulated echo DOSY pulse sequence with bipolar and spoil gradients. Apparent diffusion coefficients were obtained applying an algorithm based on the inverse Laplace transform stabilized by maximum entropy. Chemical shifts are reported to tetramethylsilane (TMS) as internal standard for both ^{1}H and ^{13}C spectra, and neat nitromethane (NM) for ^{1}H{^{15}N}HMBC spectra.

Single crystal X-ray diffraction

The single-crystal X-ray diffraction data were collected on a Bruker Apex Duo diffractometer with molybdenum radiation

(MoK_α, λ = 0.71073 Å) by doing ϕ and ω scans of narrow (0.5°) frames at 150, 210, 220 or 230 K. The empirical absorption correction was applied using the SADABS program.[35] The structures were solved by direct methods and refined by full-matrix least-squares treatment against $|F|^2$ in anisotropic approximation with SHELX 2014/7 set[36] using ShelXle program.[37] Crystallographic data including more details on the crystal structure determinations have been deposited at the Cambridge Crystallographic Data Centre: CCDC-2191672 (**[$(Mo_2O_2S_2)_2(L^4)_2$]**), CCDC-2191673 (**[$(Mo_2O_2S_2)_2(L^6)_2$]**), CCDC-2191674 (**[$(Mo_2O_2S_2)_2(L^5)_2$]**), CCDC-2191675 (**[$Mo_2O_2S_2(L^1)$]**), CCDC-2191676 (**[$Mo_2O_2S_2(L^3)$]**), CCDC-2194036 (**[$Mo_2O_2S_2(L^2)$]**).

Synthetic procedures

The ligands H_2L^1-H_2L^3 have been obtained in two steps (scheme 3): i) synthesis of 2-[4-(2-formylphenoxy)butoxy] benzaldehyde[38] and ii) condensation of dialdehyde following a general procedure. The mixture of 596 mg (2 mmol) of 2-[4-(2-formylphenoxy)butoxy]benzaldehyde, 524 or 780 mg (4 mmol) N-allyl or N-2,3-dimethylphenyl-thiosemicarbazide and 5 drops of glacial acetic acid as catalyst, in methanol (50 mL) was refluxed during 6 h. The obtained white or yellow precipitate was filtrated off, washed with methanol and dried under vacuum.

2,2'-(((Butane-1,4-diylbis(oxy))bis(2,1-phenylene))bis (methanylylidene))bis(hydrazinecarbothioamide) (H_2L^1). White powder. Yield 87%. FT-IR (ATR, ν cm^{-1}): 2187 (vw), 2050 (vw), 2017 (vw), 1990 (vw), 1596 (s), 1520 (s), 1487 (m), 1448 (m), 1385 (w), 1359 (m), 1289 (m), 1249 (s), 1194 (w), 1158 (w), 1116 (w), 1075 (m), 1044 (m), 978 (m), 954 (w), 872 (w), 834 (w), 817 (w), 756 (m), 689 (w), 646 (vw), 603 (vw), 555 (w), 485 (w), 426 (w). ^{1}H NMR (δ ppm, 400 MHz, DMSO-d_6): 11.45 (s, 2H), 8.50 (s, 2H), 8.36 (s, 2H), 8.11 and 7.90 (s, 4H), 8.07 (d, 2H), 7.35 (t, 2H), 7.06 (d, 2H), 6.94 (t, 2H), 4.11 (s, 4H), 1.99 (s, 4H). ^{13}C NMR (δ ppm, 300 MHz, DMSO-d_6): 177.64, 157.16, 138.27, 131.29, 125.94, 122.21, 120.49, 112.45, 67.64, 25.47. ESI-MS: m/z found 446.15, m/z calculated for molecular ion $[M+H]^+$ 445.59

2,2'-(((Butane-1,4-diylbis(oxy))bis(2,1-phenylene))bis (methanylylidene))bis(N-allyl-hydrazinecarbothioamide) (H_2L^2). Yellow powder. Yield, 97%. FT-IR (ATR, ν cm^{-1}): 3433 (s), 3347 (m), 3251 (s), 3147 (s), 2983 (m), 1599 (s), 1544 (s), 1525 (m), 1452 (m), 1378 (w), 1360 (w), 1281 (m), 1245 (m), 1159 (vw), 1122 (vw), 1099 (vw), 1069 (vw), 1045 (w), 1007 (vw), 940 (vw), 884 (vw), 829 (w), 790 (vw), 743 (w), 667 (vw), 614 (vw), 551 (vw), 478 (w). ^{1}H NMR (δ ppm, 400 MHz, DMSO-d_6): 11.56 (s, 2H), 8.62 (m, 2H), 8.52 (s, 2H), 8.10 (d, 2H), 7.36 (t, 2H), 7.08 (d, 2H), 6.96 (t, 2H), 5.90 (m, 2H), 5.11 (d, 4H), 4.17 (d, 8H), 2.00 (s, 4H).

2,2'-(((Butane-1,4-diylbis(oxy))bis(2,1-phenylene))bis(methany-lylidene))bis(N-2,3-dimethylphenyl-hydrazinecarbothioamide) (H_2L^3). Yellow powder. Yield, 84%. FT-IR (ATR, ν cm^{-1}): 3328 (s), 3145 (s, br), 3069 (w), 2997 (m, br), 2924 (w), 1603 (m), 1588 (m), 1554 (s), 1516 (m), 1486 (w), 1475 (m), 1455 (m), 1403 (m), 1324 (w, br), 1288 (m), 1257 (m), 1227 (m), 1177 (w), 1154 (w), 1114 (vw), 1097 (w), 1080 (w), 1062 (vw), 1041 (w), 1006 (vw), 974 (vw), 948 (w), 849 (vw), 829 (vw), 778 (w), 746 (m), 648 (vw), 590 (vw), 558 (vw), 480 (vw). ^{1}H NMR (δ ppm, 400 MHz, DMSO-d_6): 11.78 (s, 2H), 9.9 (s, 2H), 8.60 (s, 2H), 8.23 (d, 2H), 7.37 (t, 2H), 7.01 (s, 8H), 6.94 (t, 2H), 4.15 (s, 4H), 2.23 (s, 6H), 2.09 (s, 6H), 2.03 (s, 4H). ESI-MS: m/z found 654.28, m/z calculated for molecular ion $[M+H]^+$ 653.89

The synthesis of H_2L^4-H_2L^6 ligands have been performed following the same procedure as for H_2L^1-H_2L^3 using 5-(*tert*-butyl)isophthalaldehyde obtained in two steps from 5-(*tert*-butyl)isophthalic acid[39,40] (see scheme 3).

2,2'-[(5-tert-Buthyl-1,3-phenylene)dimethylidyne]bis(hydrazine carbothioamide) (H_2L^4). White powder. Yield 94%. FT-IR (ATR, ν cm^{-1}): 3266 (s, br), 3149 (s, br), 2965 (s.), 1691(vw), 1585 (s), 1525 (vs), 1443 (m), 1352(m), 1248 (m), 1229 (m), 1171 (w), 1093 (m), 991 (vw), 943 (w), 919 (vw), 877 (w), 826 (m), 696 (w), 613 (vw), 537 (vw). ^{1}H NMR (δ ppm, 400 MHz, DMSO-d_6): 11.48 (s, 2H), 8.23 and 8.09 (s, 2H), 8.05 (s, 2H), 8.02 (s, 1H), 7.75 (s, 2H), 1.33 (s, 9H). ^{13}C NMR (δ ppm, 300 MHz, DMSO-d_6): 177.86, 151.79, 142.10, 134.40, 125.65, 123.24, 34.65, 31.00. ESI-MS: m/z found 337.49, calculated for molecular ion $[M+H]^+$ 338.13.

2,2'-[(5-tert-Buthyl-1,3-phenylene)dimethylidyne]bis(N-methyl-hydrazinecarbothioamide) (H_2L^5). White powder. Yield 83%. FT-IR (ATR, ν cm^{-1}): 3287 (w), 3145 (m), 3002 (m), 2939 (m), 1547 (vs), 1524 (vs), 1471 (vw), 1439 (vw), 1393 (w), 1358 (w), 1331 (w), 1257 (m), 1711 (w), 1097 (m), 1042 (m), 941 (m), 900 (vw), 866 (w), 802 (w), 700 (w), 691 (w), 624 (w), 588 (vw), 552 (w), 494 (vw). ^{1}H NMR (δ ppm, 400 MHz, DMSO-d_6): 11.57 (s, 2H), 8.52 (m, 2H), 8.07 (s, 3H), 7.70 (s, 2H), 3.05 (d, 6H), 1.34 (s, 9H). ^{13}C NMR (δ ppm, 300 MHz, DMSO-d_6): 179.00, 152.50, 135.31, 125.70, 123.50, 30.90. ESI-MS: m/z found 365.54, calculated for molecular ion $[M+H]^+$ 366.16.

2,2'-[(5-tert-Buthyl-1,3-phenylene)dimethylidyne]bis(N-2,3-dimethylphenyl-hydrazinecarbothioamide) (H_2L^6). White powder. Yield 87%. FT-IR (ATR, ν cm^{-1}): 3333 (w), 3311 (w), 3138 (m), 2976 (m), 1605 (vw), 1583 (w), 1538 (vs), 1515 (vs), 1502 (s), 1474 (w), 1432 (w), 1406 (w), 1326 (m), 1274 (m), 1257 (w), 1230 (s), 1185 (w), 1096 (m), 1085 (w), 993 (vw), 940 (m), 896 (vw), 866 (vw), 836 (vw), 788 (w), 778 (w), 733 (m), 708 (w), 696 (w), 626 (vw), 583 (vw), 514 (vw), 434 (vw). ^{1}H NMR (δ ppm, 400 MHz, DMSO-d_6): 11.82 (s, 2H), 9.93 (s, 2H), 8.16 (s, 2H), 8.14 (s, 1H), 7.85 (s, 2H), 7.14-7.09 (m, 6H), 2.26 (s, 6H), 2.08 (s, 6H), 1.34 (s, 9H). ^{13}C NMR (δ ppm, 300 MHz, DMSO-d_6): 178.06, 152.46, 142.86, 138.39, 137.23, 135.24, 134.27, 128.31, 126.53, 125.29, 124.00, 30.92, 19.91, 13.90. ESI-MS: m/z found 546.26, calculated for molecular ion $[M+H]^+$ 545.80.

ARTICLE

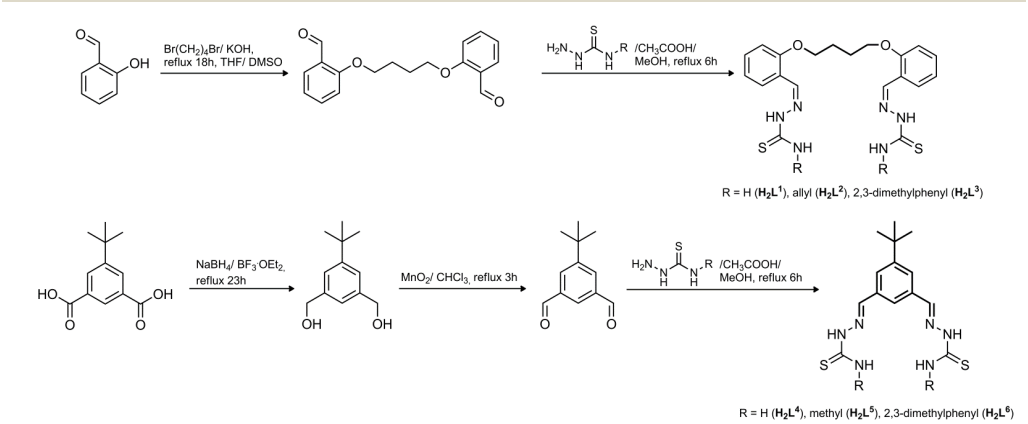

Scheme 3. The synthesis of bis-thiosemicarbazone ligands with flexible and rigid spacers

General procedure for synthesis of the complexes.
To 40 mL of a DMF or DMSO solution containing 0.833 mmol of H_2L^1-H_2L^6, 20 mL of aqueous solution containing 0.166 mmol of $K_{2-x}(NMe_4)_x[I_2Mo_{10}O_{10}S_{10}(OH)_{10}(H_2O)_5]\cdot 20H_2O$ (0.833 mmol of cluster $[Mo_2O_2S_2]^{2+}$) was added dropwise. The obtained yellow solution is heated at 80-90˚C during one hour and then cooled to room temperature. The obtained yellow powders, excepted for $[Mo_2O_2S_2(L^2)]$, were filtered, washed with ethanol, diethyl ether and dried under vacuum. Single crystals suitable for X-ray diffraction have been obtained for all complexes, except for $[Mo_2O_2S_2(L^2)]$, by slow diffusion of EtOH in NMR tubes: water mixture (1/1 v/v) in DMSO or DMF solutions of complexes. The single crystals of **$[Mo_2O_2S_2(L^2)]$** were obtained after few days by slow evaporation of mother solution. The elemental analysis (C, H, N, S), FT-IR, MALDI-TOF and NMR experiments were performed on the powders obtained after reaction and on the crystals for $[Mo_2O_2S_2(L^2)]$ complex.

$[Mo_2O_2S_2(L^1)]$. Yield 82%. FT-IR (ATR, ν cm^{-1}): 3265 (m), 3067 (s, br), 2913 (w), 1634 (m, br), 1599 (vw), 1539 (s), 1487 (m), 1455 (m), 1432 (w), 1400 (vw), 1346 (m), 1302 (m), 1248 (m), 1197 (vw), 1158 (w), 1117 (w, br), 1046 (m), 1012 (m), 963 (m), 950 (m), 819 (w), 752 (w), 659 (w), 561 (vw), 561 (vw), 480 (vw), 455 (vw). ^{1}H NMR (δ ppm, 400 MHz, DMSO-d_6): 9.65 (s, 2H), 9.08 (s, 4H), 8.29 (d, 2H), 7.43 (t, 2H), 7.15 (d, 2H), 7.01 (t, 2H), 4.20 (d, 4H), 2.00 (d, 4H). Anal. calc. for $[Mo_2O_2S_2(L^1)]\cdot(DMSO)_{2.3}(EtOH)_{0.3}$: C, 32.75; H, 4.10; N, 9.09; S, 21.86; Found C, 32.82; H, 3.57; N, 8.76; S, 22.00. EDX expected (found): Mo/S = 0.50 (0.50). MALDI-TOF: m/z calc. (found) 731.5 (730.8) for molecular ion $[M+H]^+$ and 753.5 (752.8) for molecular ion $[M+Na]^+$.Formula found by X-ray diffraction: $[Mo_2O_2S_2(L^1)]\cdot 2DMF$.

$[Mo_2O_2S_2(L^2)]$. Yield 75%. FT-IR (ATR, ν cm^{-1}): 3367 (m), 3151 (s), 3078 (vw), 2987 (m), 2876 (w), 1607 (m), 1537 (s), 1505 (m), 1486 (m), 1455 (m), 1396 (vw), 1378 (vw), 1349 (w), 1312 (w), 1289 (m), 1252 (m), 1222 (m, br), 1156 (w), 1114 (vw), 1070 (w), 1042 (w), 971 (w), 940 (vw), 901 (vw), 835 (vw), 740 (m), 604 (w, br). ^{1}H NMR (δ ppm, 400 MHz, DMSO-d_6): 9.70 (s, 4H), 8.33 (d, 2H), 7.45 (t, 2H), 7.15 (d, 2H), 7.03 (t, 2H), 5.91 (m, 2H), 5.20 (m, 4H), 4.21 (m, 4H), 4.06 (d, 4H), 2.13-1.95 (d, 4H). Anal. calc. for $[Mo_2O_2S_2(L^2)]$: C, 38.52; H, 3.73; N, 10.37; S, 15.82; Found C, 38.47; H, 3.24; N, 10.40; S, 15.80. EDX expected (found): Mo/S = 0.50 (0.50). MALDI-TOF: m/z calc. (found) 811.7 (811.9) for molecular ion $[M+H]^+$ and calc. (found) 833.6 (833.9) for molecular ion $[M+Na]^+$. Formula found by X-ray diffraction: $[Mo_2O_2S_2(L^2)]\cdot 3DMF$.

$[Mo_2O_2S_2(L^3)]$. Yield 78 %. FT-IR (ATR, ν cm^{-1}): 2919 (w, br.), 1665 (w), 1600 (w), 1551 (s), 1488 (vw), 1471 (vw), 1452 (w), 1384 (w), 1345 (m), 1250 (m), 1160 (vw), 1096 (vw), 1073 (vw), 1042 (m, br), 965 (s), 835 (vw), 756 (w), 723 (w), 663 (w), 480 (vw). ^{1}H NMR (δ ppm, 400 MHz, DMSO-d_6): 11.06 (s, 2H), 9.82 (s, 2H), 8.46 (d, 2H), 7.46 (t, 2H), 7.20 (m, 8H), 7.03 (t, 2H), 4.25 (m, 4H), 2.30 (s, 6H), 2.13 (s, 6H), 1.99-2.17 (d, 4H). Anal. calc. for $[Mo_2O_2S_2(L^3)]\cdot(DMSO)_{1.5}\cdot(H_2O)_2$: C, 42.89; H, 4.71; N, 7.70; S, 16.15; Found C, 42.73; H, 3.66; N, 7.55; S, 15.80. EDX expected (found): Mo/S = 0.50 (0.50). MALDI-TOF: m/z calc. (found) 939.8 (939.9) for molecular ion $[M+H]^+$ and 961.8 (961.9) for molecular ion $[M+Na]^+$. Formula found by X-ray diffraction: $[Mo_2O_2S_2(L^3)]\cdot 2EtOH$.

$[(Mo_2O_2S_2)_2(L^4)_2]$. Yield 90%. FT-IR (ATR, ν cm^{-1}): 3431 (m), 3308 (m, br), 3180 (w), 2965 (m), 2866 (w), 1601 (vs), 1514 (m), 1365 (m), 1344 (m), 1229 (w), 1175 (w), 1101 (w), 1053 (w), 961 (s), 808 (w), 716 (w), 694 (vw), 513 (vw), 479 (vw), 453 (vw). ^{1}H NMR (δ ppm, 400 MHz, DMSO-d_6): 9.29 (d, 6H), 8.43 (s, 2H), 8.23 (s, 1H), 1.40 (s, 9H). Anal. calc. for $[(Mo_2O_2S_2)_2(L^4)_2]\cdot(Mo_{12}O_{12}S_{12}(OH)_{12}(H_2O)_6)_{0.062}\cdot(EtOH)_{2.13}$: C, 26.15; H, 3.59; N, 11.75; S, 18.82; Found C, 26.37; H, 3.45; N, 11.45; S, 19.08. EDX expected (found): Mo/S = 0.50 (0.50). MALDI-TOF: m/z calc. (found) 1245.9 (1245.6) for molecular ion $[M+H]^+$ and calc.

(found) 1267.9 (1267.6) for molecular ion $[M+Na]^+$. Formula found by X-ray diffraction: $[(Mo_2O_2S_2)_2(L^4)_2]\cdot 5DMF\cdot 3H_2O$.

$[(Mo_2O_2S_2)_2(L^5)_2]$. Yield 88%. FT-IR (ATR, ν cm^{-1}): 3324 (m, br), 2964 (m), 1588 (vs), 1431 (vw), 1348 (m), 1229 (w), 1170 (vw), 1072 (m), 957 (s), 874 (vw), 803 (vw), 696 (w), 672 (vw), 563 (vw), 479 (vw), 418 (vw). ^1H NMR (δ ppm, 400 MHz, DMSO-d_6): 9.50 (q, 2H), 9.27 (s, 2H), 8.37 (s, 2H), 8.24 (s, 1H), 3.08 (d, 6H), 1.42 (s, 9H). Anal. calc. for $[(Mo_2O_2S_2)_2(L^5)_2]\cdot(Mo_{12}O_{12}S_{12}(OH)_{12}(H_2O)_6)_{0.03}\cdot(H_2O)\cdot(EtOH)_{0.9}$: C, 43.35; H, 4.32; N, 10.60; S, 14.70; Found C, 43.51; H, 4.34; N, 10.37; S, 14.87. EDX expected (found): Mo/S = 0.50 (0.50). MALDI-TOF: m/z calc. (found) 1302.0 (1302.7) for molecular ion $[M+H]^+$ and calc. (found) 1324.0 (1324.7) for molecular ion $[M+Na]^+$. Formula found by X-ray diffraction: $[(Mo_2O_2S_2)_2(L^5)_2]\cdot 3DMF\cdot EtOH\cdot H_2O$.

$[(Mo_2O_2S_2)_2(L^6)_2]$. Yield 98%. FT-IR (ATR, ν cm^{-1}): 3299 (w, br), 2962 (w), 2862 (w), 1664 (m), 1604 (w), 1584 (w), 1546 (vs), 1473 (w), 1382 (w), 1356 (w), 1323 (w), 1244 (w), 1190 (vw), 1095 (w), 965 (m), 817 (vw), 827 (vw), 804 (vw), 720 (m), 617 (vw), 529 (vw), 481 (vw). ^1H NMR (δ ppm, 400 MHz, DMSO-d_6): 11.12 (s, 2H), 9.45(s, 2H), 8.54 (s, 2H), 8.38 (s, 1H), 7.27 (m, 6H), 2.32 (s, 6H), 2.18 (s, 6H), 1.43 (s, 9H). Anal. calc. for $[(Mo_2O_2S_2)_2(L^6)_2]\cdot(Mo_{12}O_{12}S_{12}(OH)_{12}(H_2O)_6)_{0.008}\cdot(EtOH)_{0.1}\cdot(C_3H_7ON)_{0.8}\cdot(C_{30}H_{36}N_6S_2)_{0.045}$: C, 43.35; H, 4.32; N, 10.60; S, 14.70; Found C, 43.51; H, 4.34; N, 10.37; S, 14.87. EDX expected (found): Mo/S = 0.50 (0.50). MALDI-TOF: m/z calc. (found) 1662.5 (1662.9) for molecular ion $[M+H]^+$ and calc. (found) 1684.5 (1684.9) for molecular ion $[M+Na]^+$. Formula found by X-ray diffraction: $[(Mo_2O_2S_2)_2(L^6)_2(DMSO)_2]\cdot 7.5DMSO\cdot 3.25H_2O$.

Results and discussion

Synthesis

The bis-thiosemicarbazone ligands with flexible and rigid spacers were obtained in two or three steps according to reported procedures.[38-40] They were characterized by ESI-MS, FT-IR and NMR spectroscopy, confirming their structures and purity, and were used without further purification.

The **$[Mo_2O_2S_2(L^{1-3})]$** and **$[(Mo_2O_2S_2)_2(L^{4-6})_2]$** coordination complexes were synthesized by reaction of $K_{2-x}(NMe_4)_x[I_2Mo_{10}O_{10}S_{10}(OH)_{10}(H_2O)_5]\cdot 20H_2O$ (notated Mo_{10} precursor) with the corresponding tetradentate ligands in $[Mo_2O_2S_2]^{2+}$/ligand ratio equal to 1 using DMSO/H_2O or DMF/H_2O as solvent. In these reaction conditions, the 10 hydroxo bridges of the Mo_{10} precursor are basic enough to react with the acidic azomethinic protons of the ligands. This process led to five $[(Mo_2O_2S_2)_2(H_2O)_6]^{2+}$ clusters that are able to react with twice deprotonated thiosemicarbazone ligands. According to the crystallographic structures, the coordination occurs through the substitution of water molecules in equatorial positions through thiolate and azomethinic N atoms, giving the corresponding Mo^V based complexes. Elemental analysis (C, H, N, S), EDX measurements, and FT-IR and NMR spectroscopies are in good agreement with the expected structures. Note that the Mo_{10} precursor can evolve into the poorly soluble neutral cycle $[Mo_{12}O_{12}S_{12}(OH)_{12}(H_2O)_6]\cdot 20H_2O$, which can be found as impurity in some powders. All MALDI-TOF spectra were performed on powders in the positive mode as described in the experimental section. For each species, mainly two isotopic massifs corresponding to the protonated or sodium-cationized species are obtained (see Fig. 1, Table 1 and Figs. S1-S5). Interestingly, these massifs are assigned to the neutral dinuclear species **$[Mo_2O_2S_2(L^{1-3})]$** ($+H^+$ or $+Na^+$) when flexible spacers are used and to tetranuclear complexes **$[(Mo_2O_2S_2)_2(L^{4-6})_2]$** when bis-thiosemicarbazones with rigid spacers are involved. This feature evidences the great influence of the design of the ligand on the nuclearity of the assembly.

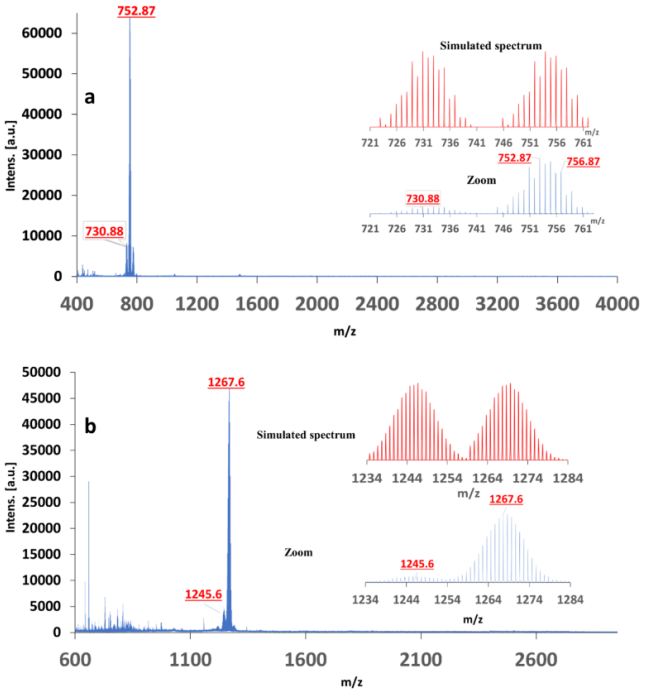

Figure 1. MALDI-TOF spectra for a) **$[Mo_2O_2S_2(L^1)]$** and b) **$[(Mo_2O_2S_2)_2(L^4)_2]$** complexes. Inset: zoomed-in section of the peak assigned to $[M+H]^+$ and $[M+Na]^+$ species in comparison with the simulated spectrum calculated with IsoPro3 software.

Table 1. MALDI-TOF results for $[Mo_2O_2S_2(L^{1-3})]$ and $[(Mo_2O_2S_2)_2(L^{4-6})_2]$ complexes

Complexes	Experimental m/z	Assignment (calcd m/z)
$[Mo_2O_2S_2(L^1)]$	730.8	$[M+H]^+$ (731.5)
	752.8	$[M+Na]^+$ (753.5)
$[Mo_2O_2S_2(L^2)]$	811.9	$[M+H]^+$ (811.7)
	833.9	$[M+Na]^+$ (833.6)
$[Mo_2O_2S_2(L^3)]$	939.9	$[M+H]^+$ (939.8)
	961.9	$[M+Na]^+$ (961.8)
$[(Mo_2O_2S_2)_2(L^4)_2]$	1245.6	$[M+H]^+$ (1245.9)
	1267.6	$[M+Na]^+$ (1267.9)
$[(Mo_2O_2S_2)_2(L^5)_2]$	1302.7	$[M+H]^+$ (1302.0)
	1324.7	$[M+Na]^+$ (1324.0)
$[(Mo_2O_2S_2)_2(L^6)_2]$	1662.9	$[M+H]^+$ (1662.5)
	1684.9	$[M+Na]^+$ (1684.5)

Single crystal structure analysis

Single crystals of all complexes were obtained. The crystallographic data are gathered in Tables 2 and 3, while selected distances are listed in Table 4.

ARTICLE

Table 2. Crystallographic data for complexes **$[Mo_2O_2S_2(L^1)]$**, **$[Mo_2O_2S_2(L^2)]$** and **$[Mo_2O_2S_2(L^3)]$**

Complex	**$[Mo_2O_2S_2(L^1)]$**	**$[Mo_2O_2S_2(L^2)]$**	**$[Mo_2O_2S_2(L^3)]$**
Formula	$C_{26}H_{36}Mo_2N_8O_6S_4$	$C_{35}H_{51}Mo_2N_9O_7S_4$	$C_{39}H_{47}Mo_2N_6O_6S_4$
M (g mol^{-1})	876.75	1029.97	1015.94
Temperature	210	150	210
Crystal system	Orthorhombic	Triclinic	Triclinic
Space group	*Pbca*	*P*-1	*P*1
a (Å)	14.4020(4)	9.8604(4)	11.2201(6)
b (Å)	18.8426(5)	11.8441(5)	12.1164(6)
c (Å)	27.1560(8)	21.7263(9)	18.3239(9)
α (°)	90	74.869(2)	76.257(2)
β (°)	90	79.023(2)	87.948(2)
γ (°)	90	65.735(2)	88.316(2)
V (Å^3)	7369.4(4)	2223.01(16)	2417.7(2)
Z	8	2	2
D_{calc}	1.580	1.539	1.396
Crystal size (mm)	0.30 × 0.20 × 0.06	0.31 × 0.17 × 0.14	0.20 × 0.12 × 0.04
F(000)	3552	1056	1038
μ (Mo-Kα)/mm^{-1}	0.71073	0.71073	0.71073
Reflections collected	486382	112483	158731
Independent reflections (I > 2σ(I))	10137	17397	11937
Parameters	419	520	563
Δ(ρ) (e Å^{-3})	0.48 and -0.46	1.379 and -0.947	1.70 and -0.61
Goodness of fit	1.14	1.212	1.11
R1[a]	0.0215 (0.024)[b]	0.0289 (0.0363)[b]	0.0333 (0.0434)[b]
wR2[a]	0.0509 (0.0526)[b]	0.0579 (0.0625)[b]	0.0974 (0.107)[b]

[a]$R = \sum||F_o| - |F_c||/\sum|F_o|$, $wR_2 = [\sum w(F_o^2 - F_c^2)^2/\sum w(F_o^2)^2]^{1/2}$; [$F_o > 4\sigma(F_o)$]. [b]Based on all data.

Table 3 Crystallographic data for complexes **$[(Mo_2O_2S_2)_2(L^4)_2]$**, **$[(Mo_2O_2S_2)_2(L^5)_2]$** and **$[(Mo_2O_2S_2)_2(L^6)_2]$**

Complex	**$[(Mo_2O_2S_2)_2(L^4)_2]$**	**$[(Mo_2O_2S_2)_2(L^5)_2]$**	**$[(Mo_2O_2S_2)_2(L^6)_2]$**
Formula	$C_{40}H_{64}Mo_4N_{16}O_{9.50}S_8$	$C_{41.50}H_{67.50}Mo_4N_{14.50}O_{8.25}S_8$	$C_{79}H_{125}Mo_4N_{12}O_{16.75}S_{17.50}$
M (g mol^{-1})	1561.31	1541.84	2455.71
Temperature	230	210	220
Crystal system	Triclinic	Triclinic	Triclinic
Space group	*P*1	*P*1	*P*1
a (Å)	14.458(1)	14.7740(7)	15.1256(5)
b (Å)	15.6676(9)	15.8521(7)	19.0607(6)
c (Å)	16.4741(11)	17.0582(9)	21.7932(11)
α (°)	88.655(3)	66.431(2)	91.701(3)
β (°)	73.617(3)	67.927(2)	95.393(3)
γ (°)	70.679(2)	68.124(2)	108.581(2)
V (Å^3)	3368.5(4)	3275.0(3)	5917.4(4)
Z	2	2	2
D_{calc}	1.539	1.564	1.378
Crystal size (mm)	0.22 × 0.14 × 0.04	0.24 × 0.16 × 0.12	0.30 × 0.06 × 0.04
F(000)	1576	1560	2530
μ (Mo-Kα)/mm^{-1}	0.71073	0.71073	0.71073
Reflections collected	133440	185221	357366
Independent reflections (I > 2σ(I))	16036	15880	22742
Parameters	767	721	1214
Δ(ρ) (e Å^{-3})	2.20 and -1.10	1.18 and -0.80	1.79 and -1.74

Goodness of fit	1.08	1.10	1.07
R1[a]	0.0665 (0.0984)[b]	0.0344 (0.0517)[b]	0.0628 (0.077)[b]
wR2[a]	0.1874 (0.212)[b]	0.0851 (0.0982)[b]	0.1759 (0.1972)[b]

[a]$R = \sum||F_o| - |F_c||/\sum|F_o|$, $wR_2 = [\sum w(F_o^2 - F_c^2)^2/\sum w(F_o^2)^2]^{1/2}$; $[F_o > 4\sigma(F_o)]$. [b]Based on all data.

Table 4. Selected bond lengths around Mo atoms (Å)

Complex	label	C-S	(N)N=C(S)	Mo-Mo	Mo-N	Mo-S_{ligand}	Mo-$S_{bridges}$	Mo=O
$[Mo_2O_2S_2(L^1)]$	Mo1	1.742	1.330	2.845	2.138	2.451	2.310, 2.314	1.677
	Mo2	1.736	1.333		2.127	2.450	2.310, 2.324	1.680
$[Mo_2O_2S_2(L^2)]$	Mo1	1.739	1.338	2.844	2.131	2.473	2.309, 2.325	1.672
	Mo2	1.746	1.336		2.116	2.455	2.319, 2.309	1.674
$[Mo_2O_2S_2(L^3)]$	Mo1	1.731	1.332	2.828	2.143	2.457	2.309, 2.328	1.671
	Mo2	1.747	1.328		2.134	2.452	2.323, 2.314	1.672
$[(Mo_2O_2S_2)_2(L^4)_2]$	Mo1	1.731	1.326	2.853	2.149	2.457	2.303, 2.324	1.667
	Mo2	1.741	1.323		2.145	2.459	2.307, 2.304	1.670
	Mo3	1.712	1.344	2.845	2.134	2.454	2.323, 2.315	1.666
	Mo4	1.743	1.330		2.144	2.460	2.316, 2.290	1.664
$[(Mo_2O_2S_2)_2(L^5)_2]$	Mo1	1.731	1.334	2.841	2.141	2.464	2.311, 2.317	1.668
	Mo2	1.740	1.333		2.123	2.459	2.318, 2.308	1.671
	Mo3	1.747	1.337	2.832	2.138	2.450	2.322, 2.288	1.681
	Mo4	1.735	1.335		2.129	2.477	2.311, 2.323	1.671
$[(Mo_2O_2S_2)_2(L^6)_2]$	Mo1	1.737	1.329	2.822	2.157	2.486	2.326, 2.341	1.678
								Mo-O_{DMSO} : 2.501
	Mo2	1.730	1.325		2.158	2.456	2.320, 2.307	1.678
	Mo3	1.730	1.333	2.833	2.147	2.493	2.352, 2.326	1.680
								Mo-O_{DMSO} : 2.436
	Mo4	1.738	1.327		2.139	2.467	2.319, 2.309	1.672

Binuclear complexes with flexible spacers **$[Mo_2O_2S_2(L^1)]$**, **$[Mo_2O_2S_2(L^2)]$** and **$[Mo_2O_2S_2(L^3)]$** crystallize in P_{bca}, P-1 and P1 space groups, respectively. Tetranuclear complexes with rigid spacers, namely **$[(Mo_2O_2S_2)_2(L^4)_2]$**, **$[(Mo_2O_2S_2)_2(L^5)_2]$** and **$[(Mo_2O_2S_2)_2(L^6)_2]$** all crystallize in non-centrosymmetric P1 space group.

All Mo^V atoms in the six molecular structures appear in a distorted square pyramid geometry linked in axial positions by an oxo ligand and in equatorial positions by two μ-sulfido atoms and two donating atoms of the ligands, except for Mo1 and Mo3 in **$[(Mo_2O_2S_2)_2(L^4)_2]$**, which are in a distorted octahedral geometry. The Mo-Mo, Mo-S and Mo=O bond distances found in the ranges 2.83-2.85, 2.31-2.33 and 1.67-1.68 Å respectively, are characteristic for $[Mo_2O_2S_2]^{2+}$ cluster (Table 4).[6,7]

The asymmetric units of the three complexes with flexible spacers on the ligands, i.e. **$[Mo_2O_2S_2(L_1)]$**, **$[Mo_2O_2S_2(L^2)]$** and **$[Mo_2O_2S_2(L^3)]$**, are depicted in the Figs. 2 and 3. In the three cases the complexes involve one $[Mo_2O_2S_2]^{2+}$ cluster coordinated to a bis(bidentate) twice deprotonated (L^{2-}) bis-thiosemicarbazone ligands. On each side of the $[Mo_2O_2S_2]^{2+}$ cluster the ligands are coordinated in two equatorial positions of Mo atoms by thiolate groups and by azomethinic N atoms of the thiosemicarbazide fragments, leading to a 4-atom cycle with metal atoms. In the literature, the thiosemicarbazone ligands usually coordinate by the N-imino atoms, thion/thiolate groups and other functions.(add ref) Therefore, coordination through the azomethine N atom remains less common and appears to be specific to $[Mo_2O_2S_2]^{2+}$-based complexes.[34] The deprotonation of the ligands by Mo_{10} precursor can be evidenced through C-S and C=N bond distances (Table 4). The average C-S bond lengths found in the complexes (1.74 Å) are consistent with single C-S bonds and higher than the C=S double bond observed in the uncoordinated ligands (in the range 1.65-1.70 Å).[34] As expected, the C-N distance in complexes is shorter (1.33 Å) than in free ligands (1.35 Å)[41] thus confirming the C=N bond formation. Furthermore, the average Mo-S_{ligand} bond lengths of 2.46 Å correspond to the Mo-S distances involving Mo(V) metal ions (Table 4).[42-45]

The representation given in Fig. 2a could suggest that the complexes **$[Mo_2O_2S_2(L_1)]$**, **$[Mo_2O_2S_2(L^2)]$** and **$[Mo_2O_2S_2(L^3)]$** are relatively planar. In fact, the representation given in Fig. 2b evidences that the complexes describe a basket-handle shape. The ligands are bend through coordination to $[Mo_2O_2S_2]^{2+}$ cluster. The angles between the phenoxy fragments, 4-atom cycle with Mo metal atoms and the distances among phenoxy rings are shown in the Table S1.

Concerning the crystal packing, the thiosemicarbazone complexes are well-known to give H-bond networks between the complexes and solvates.[46] The crystal packing of our complexes was thus examined to identify these H-bond networks. The crystal packings are given in Figs. S6-S15 in the ESI.

The crystal packing of the complex **$[Mo_2O_2S_2(L^1)]$** co-crystallized with two DMF molecules, shows moderate to weak intermolecular hydrogen bonding involving molecular units and solvent molecules (Fig. S6). They can be regrouped in three category: i) Mo=O…H type between Mo=O2 and N-H groups

(N1A-H1A…O2, 2.197 Å, 146.19˚); ii) S…H type between one bridging sulfur and N-H amino group (N1B-H1C…S2, 2.773 Å, 148.36˚) and between Mo-S_{ligand} and C-H linkage of one DMF molecule (C4C-H4C…S3B, 2.900 Å, 129.05˚); iii) N-H…O type involving N-H amino groups and oxygen atoms of DMF molecules (N1A-H1B…O5D, 1.936 Å, 155.17˚; N1B-H1D…O5C, 1.919 Å, 167.27 ˚).

The compound **$[Mo_2O_2S_2(L^2)]$** is co-crystallized with three DMF molecules and present more complex hydrogen bonding networks (Fig. S7). Two types of hydrogen bond interactions can be observed: i) S…H type between bridging sulfur (S1) and one DMF molecule (C103-H107…S1, 2.792 Å, 172.61˚) and ii) NH…O type involving N-H amino groups and DMF molecules (N1B-H1B…O100, 1.947 Å, 159.28˚; N1A-H1A…O102, 1.952 Å, 145.56˚) and between two DMF molecules (C100-H100…O101, 2.380 Å, 171.83˚).

The crystal packing of **$[Mo_2O_2S_2(L^3)]$** depicted in the Fig. S8 doesn't present any kinds of particular intermolecular hydrogen bonds network.

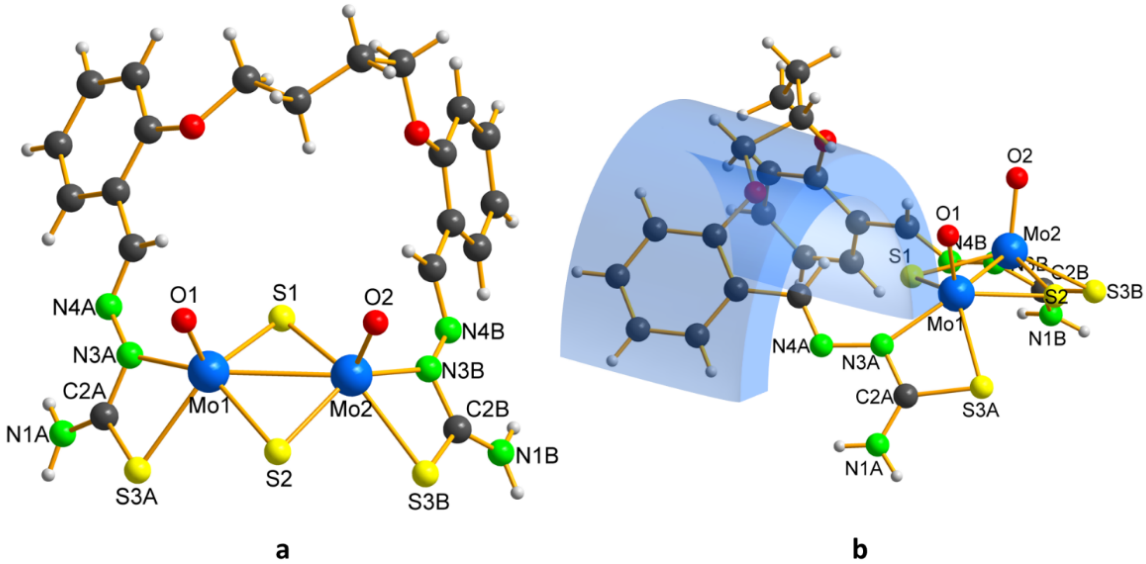

Figure 2. Molecular structure of **$[Mo_2O_2S_2(L^1)]$: a)** in front and b) lateral views. Colour code: Mo (blue), C (gray), O (red), N (green), and S (yellow).

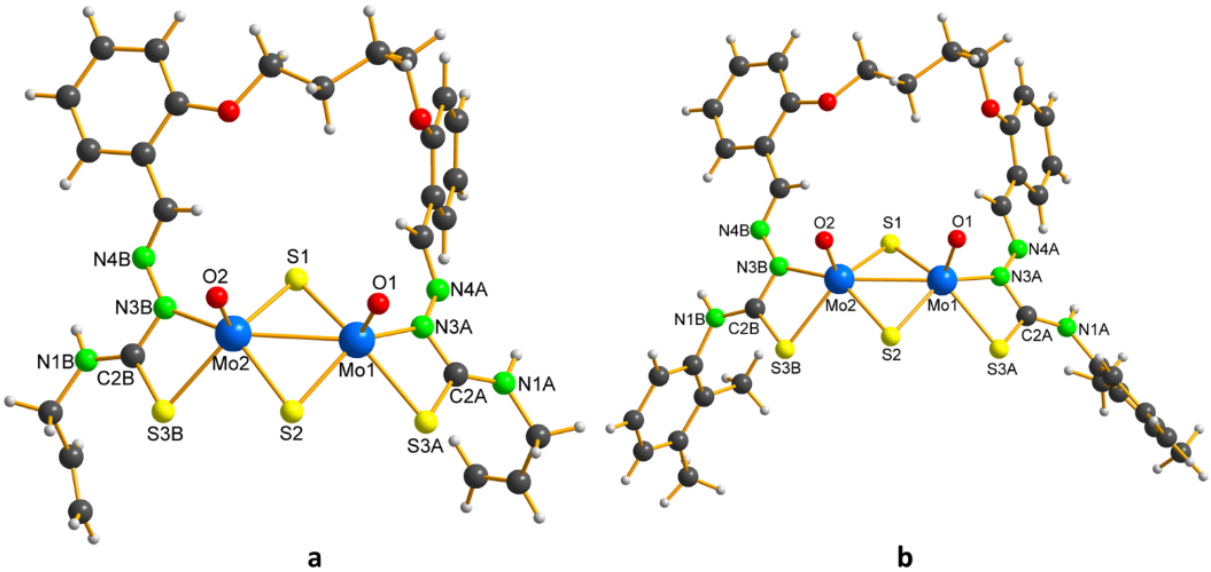

Figure 3. Molecular structures of a) **$[Mo_2O_2S_2(L^2)]$** and b) **$[Mo_2O_2S_2(L^3)]$**. Colour code: Mo (blue), C (gray), O (red), N (green), and S (yellow).

In contrast to these three complexes, the reaction of the bis-thiosemicarbazone ligands H_2L^4-H_2L^6 obtained from 5-(*tert*-butyl)-isophthalaldehyde all yield tetranuclear complexes of formulas **$[(Mo_2O_2S_2)_2(L^4)_2]$**, **$[(Mo_2O_2S_2)_2(L^5)_2]$** and **$[(Mo_2O_2S_2)_2(L^6)_2]$**, which have a rectangular shape (Figs. 4 and 5). For the three complexes, each $[Mo_2O_2S_2]^{2+}$ cluster is coordinated to two ligands and each bis-thiosemicarbazone ligand coordinates two $[Mo_2O_2S_2]^{2+}$ clusters through thiolate groups and azomethinic nitrogen atoms as previously observed with flexibles spacers. All bond distances around Mo metal ions are similar as described for the complexes with flexible spacers (see Table 4). Almost all the Mo atoms display a square

pyramidal geometry excepted the Mo1 and Mo3 metal centers in the complex **[(Mo$_2$O$_2$S$_2$)$_2$(L^6)$_2$]**, which are in a distorted octahedral coordination completed by a DMSO molecule in axial position trans from Mo=O bond. The neighboured Mo2 and Mo4 metal ions remain as usual in distorted square pyramid geometry. As with previous complexes with flexible spacers, the coordination of rigid bis-thiosemicarbazone ligands to $[Mo_2O_2S_2]^{2+}$ clusters results in folded rectangular complexes. The distances between *tert*-butylphenyl fragments and 4-atom cycle with Mo atoms plans are giving in the Table S1 (ESI).

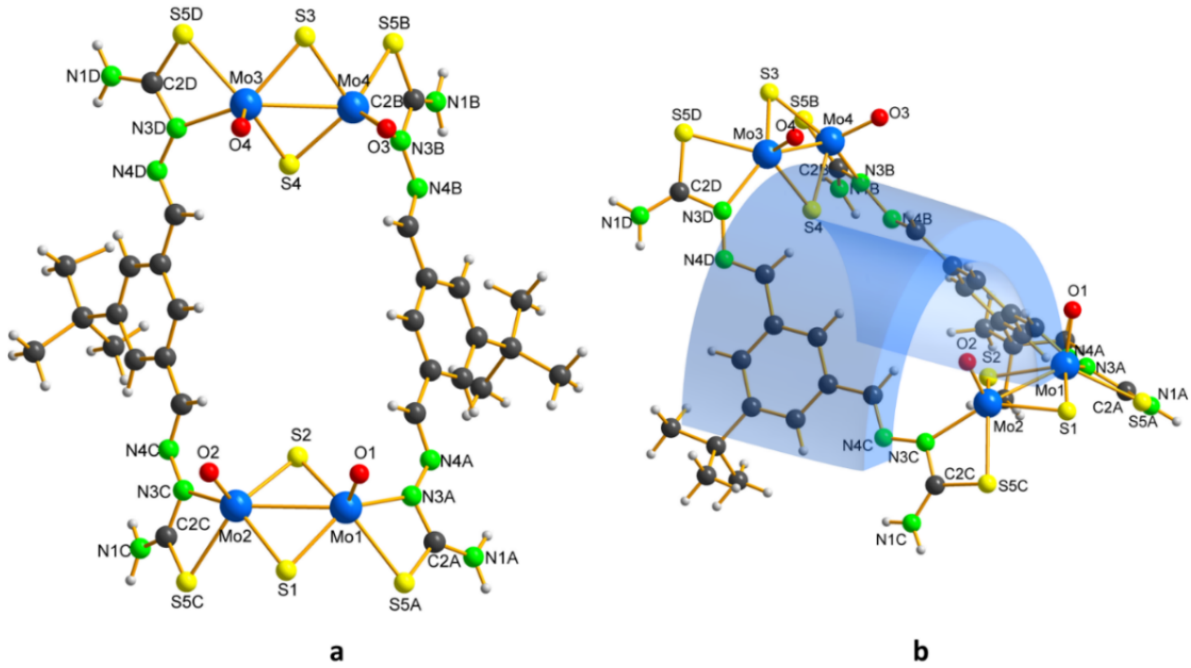

Figure 4. Molecular structure of **[(Mo$_2$O$_2$S$_2$)$_2$(L^4)$_2$]:** a) in front and b) lateral views. Colour code: Mo (blue), C (gray), O (red), N (green), and S (yellow).

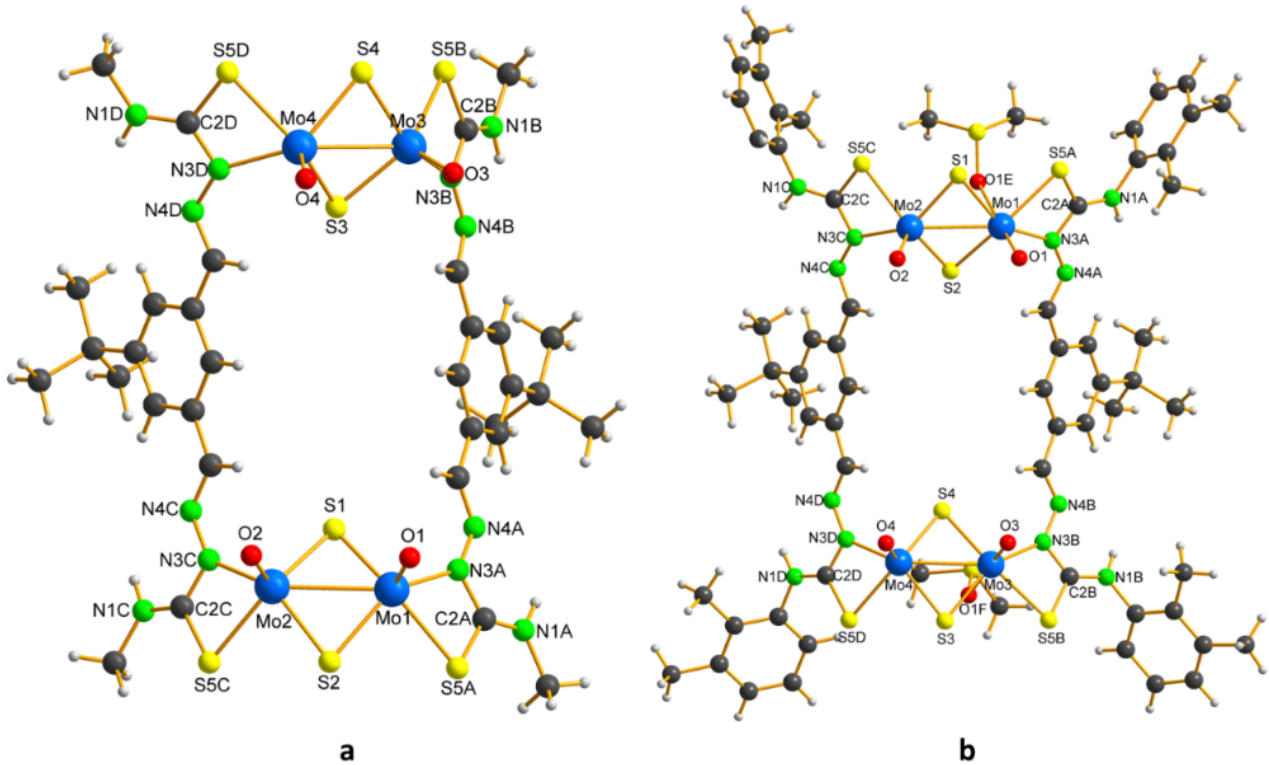

Figure 5. Molecular structures of a) **[(Mo$_2$O$_2$S$_2$)$_2$(L^5)$_2$]** and b) **[(Mo$_2$O$_2$S$_2$)$_2$(L^6)$_2$]**. Colour code: Mo (blue), C (gray), O (red), N (green), and S (yellow).

ARTICLE

The crystal packing of **[(Mo$_2$O$_2$S$_2$)$_2$(L^4)$_2$]** co-crystallized with five DMF molecules shows many intermolecular S…S and S…O interactions and also intermolecular hydrogen bonding (see Figs. S9-S11). The S…S interactions in zig-zag fashion (S5A…S1, 3.425 Å and S1…S1, 3.343 Å) involve one thiolate and one bridging sulfur atoms from Mo1Mo2 cluster of two molecular units. There are two kinds of intermolecular Mo=O…S interactions: i) between Mo1=O and thiolate sulfur atoms from Mo3Mo4 cluster (Mo1=O1…S5D, 3.155 Å) and ii) two interactions involving Mo=O linkages and bridging sulfur atoms of Mo3Mo4 clusters (Mo3=O4…S4, 3.262 Å). In addition, the crystal packing is stabilized by NH…X (X = N, O) intermolecular hydrogen bonding between two amino groups (N1C-H1C2…N1B, 2.723 Å, 114.15˚) or between amino groups and oxygen atom of DMF molecule (N1A-H1A1…O5E, 2.086 Å, 157.06˚; N1A-H1A2…O5G, 1.957 Å, 166.13˚; N1C-H1C1…O5H, 2.197 Å, 138.10˚; N1B-H1B2…O5H, 2.022 Å, 159.69˚; N1B-H1B1…O5I, 2.099 Å, 125.76˚; N1C-H1C2…O5I, 2.404 Å, 145.81˚; N1D-H1D2…O5F, 2.147 Å, 157.14˚; N1D-H1D1…O5E, 2.047 Å, 154.58˚).

The **[(Mo$_2$O$_2$S$_2$)$_2$(L^5)$_2$]** complex solvated with four DMF molecules, one EtOH molecule and one water molecule, exhibits two types of intermolecular hydrogen bonding (see Figs. S12-S13, ESI): i) NH…O type involving NH group and oxygen atoms of DMF molecules (N1C-H1C…O1E, 2.089 Å, 139.59˚; N1A-H1A…O1F, 2.031 Å, 147.18˚; N1D-H1D…O1F, 2.095 Å, 147.10˚) or EtOH (N1B-H1B…O1G, 2.044 Å, 151.29˚) and ii) Mo=O…H type, between Mo2=O and DMF molecule (C2E-H2E…O2=Mo2, 2.380 Å, 153.41˚).

Finally, as seen in Figs. S14 and S15 (ESI) the crystal packing of **[(Mo$_2$O$_2$S$_2$)$_2$(L^6)$_2$]** is stabilized by NH…O intermolecular hydrogen bonds between amino groups and oxygen atoms of DMSO molecules (N1D-H1D…O1G, 2.021 Å, 155.12˚; N1A-H1A…O1I, 2.046 Å, 154.08˚; N1C-H1C…O1J, 2.142 Å, 162.99˚; N1B-H1B…O1K, 2.076 Å, 148.72˚).

NMR studies

The NMR spectroscopy is a very important tool to investigate in solution the coordination modes, the molecular size, possible isomers or other species of $[Mo_2O_2S_2]^{2+}$-based bis-thiosemicarbazone complexes. The ^{1}H NMR, 2D ^{1}H DOSY and ^{15}N{^{1}H} HMBC measurements have been performed in DMSO-d_6. As all complexes show similar NMR behaviour we will discuss here the properties of **[Mo$_2$O$_2$S$_2$(L^1)]** (Fig. 6) and **[(Mo$_2$O$_2$S$_2$)$_2$(L^4)$_2$]** (Fig. 7) compounds as representative systems with flexible and rigid spacers, respectively. The NMR spectra for other complexes are given in the ESI (Figs. S16-S32).

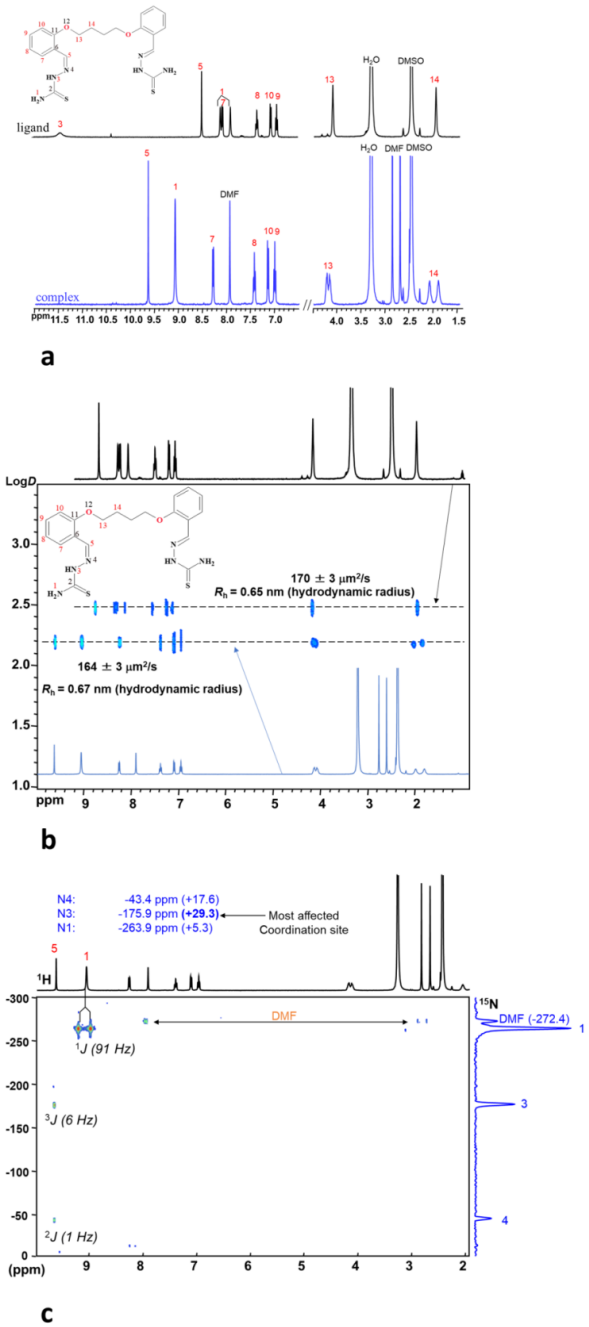

Figure 6. (a) ^{1}H-NMR spectra of H_2L^1 and **[Mo$_2$O$_2$S$_2$(L^1)]** complex; (b) ^{1}H-NMR DOSY spectra for H_2L^1 (top) and **[Mo$_2$O$_2$S$_2$(L^1)]** complex (bottom); (c) ^{1}H{^{15}N} HMBC spectrum for **[Mo$_2$O$_2$S$_2$(L^1)]** complex. The ^{15}N chemical shifts of the three N sites of the ligand N1, N3, and N4 are indicated as well as the differences from the free ligand values in parentheses.

As observed in the Fig. 6a, the ^{1}H NMR spectrum of **[Mo$_2$O$_2$S$_2$(L^1)]** displays 8 signals, while 9 resonances are seen for

the free ligand. The azomethinic N proton H3 found at 11.5 ppm in the ligand disappeared after complexation thus confirming the deprotonation of the bis-thiosemicarbazone ligands. Furthermore, all proton peaks appear downfield shifted compared to the free ligands in agreement with the coordination of the ligands. The peaks of thiosemicarbazide fragments are the most affected. Thus, the imino protons (C**H**=N) are moved by +0.65 ppm and the two singlets corresponding to thioamide protons (CS-N**H**$_2$) become equivalent and show one singlet at 9.25 ppm. No trace of free ligand or other minor species is observed in the spectrum of **[Mo$_2$O$_2$S$_2$(L^1)]**, consistent with the presence of a single molecular species in solution. This selectivity differs from previous study with mono-thiosemicarbazone ligands that gave mixtures of up to 8 isomers of 1:2 complexes.[34] Finally, the splitting of the methylene resonances (C13 and C14 in Fig.6) after complexation is consistent with the lowering of the symmetry of the ligand from C_s to C_1 as observed in the solid state, shown in Fig. 2. Similar observations are made for the two other complexes built from bis-thiosemicarbazone ligands containing flexible linker, i.e., **[Mo$_2$O$_2$S$_2$(L^2)]** and **[Mo$_2$O$_2$S$_2$(L^3)]**.

Concerning the three tetranuclear complexes synthesized with rigid ligand, the ^{1}H NMR spectrum of ligand H$_2$L^4 and complex **[(Mo$_2$O$_2$S$_2$)$_2$(L^4)$_2$]** are given in Fig. 7a. Similarly, with the previous complexes, the azomethinic protons of the ligand disappears during the complexation process. The other five types of protons of the free ligand exhibit 5 signals that undergo a deshielding effect upon complexation with the $[Mo_2O_2S_2]^{2+}$ cluster. These peaks are attributed to a single molecular species in solution with C_s symmetry fully compatible with the X-ray structure given in Fig. 4. Similar analyses are made for ligands H$_2$L^5 and H$_2$L^6 and their complexes (see ESI).

The ^{1}H DOSY NMR spectra performed on the ligands and complexes (Figs. 6b and 7b) allow to determine the diffusion coefficients of each species in solution. This technique permits to highlight the mixture of species (if any) but also to measure the hydrodynamic radii of each species.[47] The values are gathered in Table 5.

Table 5. Measured diffusion coefficients and calculated hydrodynamic radii of ligands and complexes in DMSO-d$_6$ (total concentration of ligand = 10 mM)

Compounds	D (µm^2/s)	Calculated r$_h$ hydrodynamic radii [b] (Å)
H$_2$L^1	170 ± 3	6.5
H$_2$L^2	163 ± 6	6.7
H$_2$L^3	158 ± 3	7.0
H$_2$L^4	182 ± 2	6.1
H$_2$L^5	190 ± 6	5.8
H$_2$L^6	160 ± 7	6.9
[Mo$_2$O$_2$S$_2$(L^1)]	164 ± 3	6.7
[Mo$_2$O$_2$S$_2$(L^2)]	167 ± 6	6.6
[Mo$_2$O$_2$S$_2$(L^3)]	151 ± 4	7.3
[(Mo$_2$O$_2$S$_2$)$_2$(L^4)$_2$]	132 ± 2	8.3
[(Mo$_2$O$_2$S$_2$)$_2$(L^5)$_2$]	133 ± 2	8.3
[(Mo$_2$O$_2$S$_2$)$_2$(L^6)$_2$]	134 ± 6	8.2

[a] r$_H$ are calculated using Stokes–Einstein equation D = k$_B$T/6πηr$_h$: k$_B$ Boltzmann's constant, T temperature (K), and η solvent viscosity

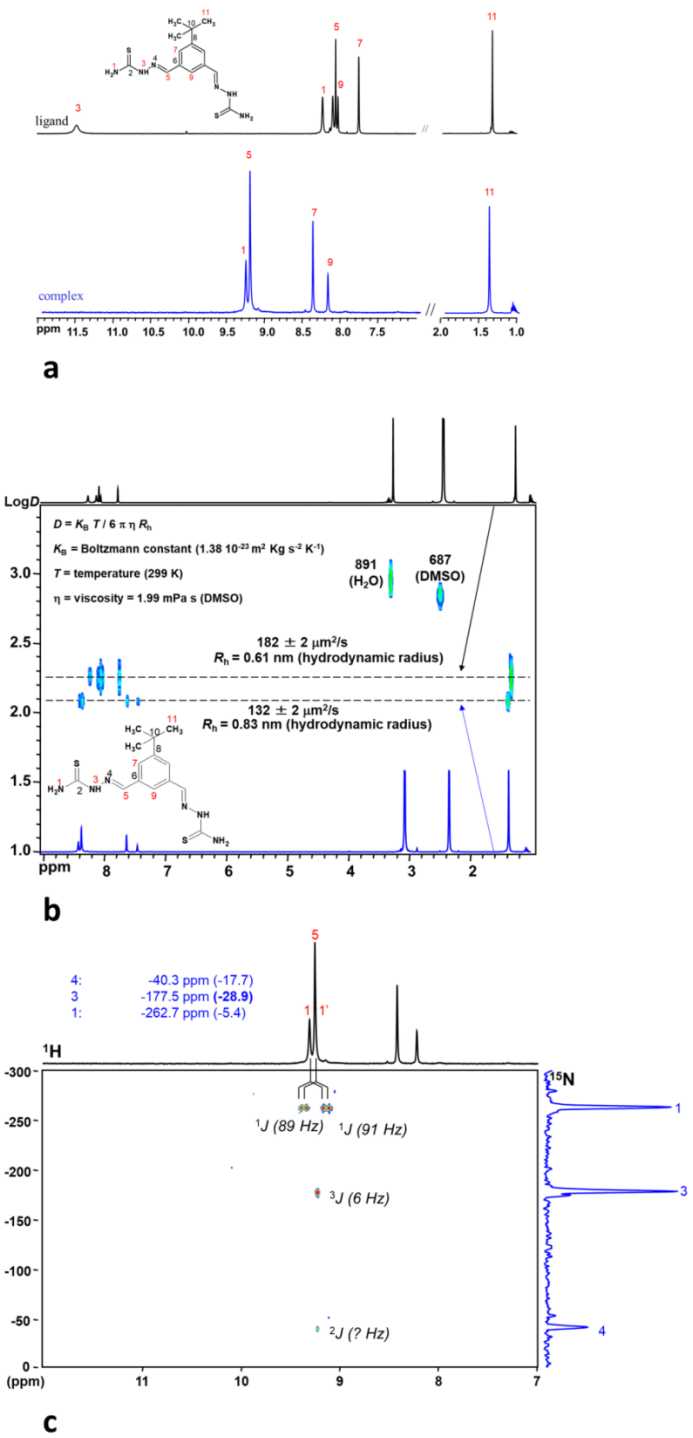

Figure 7. (a) ^{1}H-NMR spectra of H$_2$L^4 and **[(Mo$_2$O$_2$S$_2$)$_2$(L^4)$_2$]** complex; (b) ^{1}H-NMR DOSY spectra for H$_2$L^4 (top) and **[(Mo$_2$O$_2$S$_2$)$_2$(L^4)$_2$]** complex (bottom); (c) ^{1}H{^{15}N} HMBC spectrum for **[(Mo$_2$O$_2$S$_2$)$_2$(L^4)$_2$]** complex. The ^{15}N chemical shifts of the three N sites of the ligand N1, N3, and N4 are indicated as well as the differences from the free ligand values in parentheses.

For the first series of flexibles bis-thiosemicarbazone ligands the values of D fall in the range 158-170 µm^2·s^{-1} in DMSO, logically smaller than the values previously determined for

mono-thiosemicarbazone ligands (220-300 $\mu m^2 \cdot s^{-1}$ in DMSO).[34] Upon formation of complexes, the diffusion coefficients values remain close to those of uncoordinated ligands, i.e. 151-167 $\mu m^2 \cdot s^{-1}$ in DMSO in agreement with the fact that the hydrodynamic radii of complexes **$[Mo_2O_2S_2(L^1)]$**, **$[Mo_2O_2S_2(L^2)]$** and **$[Mo_2O_2S_2(L^3)]$** are not enhanced compared to the free ligands. Such a behaviour is the signature of large flexible ligands whose complexation does not change the hydrodynamic volume so much. In contrast, the diffusion coefficients of ligands H_2L^{4-6} are in the 151-167 $\mu m^2 \cdot s^{-1}$ range in DMSO and their complexes give significantly lowered D values in the range 132-134 $\mu m^2 \cdot s^{-1}$ in DMSO, which translate by hydrodynamic radii around 8.2 Å, confirming the formation of 2:2 assemblies.

Finally, the $^1H\{^{15}N\}$ HMBC NMR method offers the possibility to assign the nitrogen and related proton peaks in the complexes compared to the free ligands. As seen in the Fig. S16 for the H_2L^1 ligand, the N3 and N4 appears coupled with the H5 proton with different coupling constants of ^3J (6 Hz) and ^2J (2 Hz) at -205.2 and -61.0 ppm, respectively. The signal of the N1 atoms corresponding to terminal thioamide group (CS-N**H_2**) are the most shifted at -269.2 ppm. As the free rotation of the two terminal protons is restricted by π-delocalisation or some intramolecular interactions, they are non-equivalent and consequently show two strong coupling constants with N1 atoms: ^1J (92 Hz and 87 Hz). Through complexation, as depicted in the Fig. 6c for **$[Mo_2O_2S_2(L^1)]$** complex, all terminal thioamide protons become equivalent and are coupled with N1 through same coupling constant (^1J 90 Hz). As the N1 atom is not directly coordinated to $[Mo_2O_2S_2]^{2+}$ cluster, its position is only slightly affected by complexation appearing at -263.2 ppm. The N3 and N4 atom peaks are found at -175.9 and -43.4 ppm, respectively with the same coupling constant as in the free ligand. The N3 signal is the most shifted thus confirming its direct coordination to Mo centers in agreement with X-ray molecular structure. As shown in the Fig. 7c, the tetranuclear **$[(Mo_2O_2S_2)_2(L^4)_2]$** complex exhibit broadly similar $^1H\{^{15}N\}$ correlation characteristics to the dinuclear complex **$[Mo_2O_2S_2(L^1)]$** since they present similar coordination modes. Finally, the six complexes studied show comparable results, which are found in the ESI.

To sum up, the NMR studies fully agree with the formation of 1:1 or 2:2 species between ligands and molybdic clusters and the species observed in the solid-state are preserved in DMSO solution. It demonstrates also that the bis-thiosemicarbazone ligand with flexible spacers give exclusively the formation of 1:1 species, while 2:2 adducts are selectively obtained with rigid spacers.

Conclusions

Three binuclear $[Mo_2O_2S_2(L^{1-3})]$ and three tetranuclear $[(Mo_2O_2S_2)_2(L^{4-6})_2]$ complexes were obtained by combination of $[Mo_2O_2S_2]^{2+}$ cluster with bis-thiosemicarbazone ligands with flexible (H_2L^1-H_2L^3) or rigid (H_2L^4-H_2L^6) spacers, respectively. The twice deprotonated bis-thiosemicarbazone ligands show unusual coordination mode by thiolate S and the azomethinic N atoms. MALDI-TOF MS measurements performed on powders provide information about nuclearity and are consistent with binuclear and tetranuclear Mo^V based complexes, as revealed by X-ray structure determination. The $^1H\{^{15}N\}$ HMBC NMR technique allows us to study in solution the coordination mode of the complexes to respect to the free ligands and thus to understand the coordination behaviour of thiosemicarbazones. The ^1H DOSY NMR spectra of the complexes show all proton signals with the same diffusion coefficients corresponding to a single molecular species in agreement with X-ray structures at solid-state. These results unambiguously demonstrate that we were successful in avoiding the formation of isomers by coordination to $[Mo_2O_2S_2]^{2+}$ cluster using bis-thiosemicarbazone ligands. Furthermore, this study demonstrates that the nuclearity of the assemblies depends on the nature of the spacer in our bis-thiosemicarbazone ligands. Using flexible or rigid spacers selectively leads to 1:1 or 2:2 assemblies. Our future works will be dedicated to the study of the biological properties of these complexes and to the modification of such bis-thiosemicarbazone ligands to design even larger molecular systems.

Author Contributions

Diana Cebotari : Synthesis and characterizations; Jerôme Marrot, Régis Guillot, and Clément Falaise : X-Ray diffraction studies; Sergiu Calancea : characterization of compounds and the writing of the original draft; Vincent Guérineau, and David Touboul : MALDI-TOF experiments; Mohamed Haouas: NMR experiments; Aurelian Gulea and Sébastien Floquet: supervision of the work, funding acquisition and writing of the manuscript.

Conflicts of interest

There are no conflicts to declare.

Acknowledgements

University of Versailles and the CNRS are gratefully acknowledged for financial support. DC gratefully acknowledge Campus France for Excellence Eiffel grant as well as State University of Moldova for funding their PhD thesis. This work is also supported by the "ADI 2019" project funded by the IDEX Paris-Saclay, ANR-11-IDEX-0003-02, "a Joint research projects AUF-MECR 2020-2021" funding program, and the public grant overseen by the French National Research Agency as part of the "Investissements d'Avenir" program (Labex Charm3at, ANR-11LABX-0039-grant). The financial support from National Agency for Research and Development (ANCD) of the Republic of Moldova (Project No 20.80009.5007.10) is also acknowledged.

Notes and references

1 V. N. Gladyshev and Y. Zhang, *Abundance, Ubiquity and Evolution of Molybdoenzymes*. In Molybdenum and Tungsten Enzymes; RSC, 2017, Chapter 2, pp 81−99.
2 L. B. Maia, I. Moura and J. J. G. Moura, *Molybdenum and Tungsten-Containing Enzymes: An Overview.* In Molybdenum and Tungsten Enzymes; RSC, 2017, Chapter 1, pp 1−80.
3 M. L. Kirk, *Spectroscopic and Electronic Structure Studies of Mo Model Compounds and Enzymes*. In Molybdenum and Tungsten Enzymes; RSC, 2017, Chapter 2, pp 13−59.
4 V. R. Ott, D. S. Swieter and F. A. Schultz, *Inorg. Chem. 1977*, **16**, 2538.
5 B. Spivak, Z. Dori, *Coord. Chem. Rev.* **1975**, *17*, 99.
6 E. Cadot, M. N. Sokolov, V. P. Fedin, C. Simonnet-Jegat, S. Floquet, F. Secheresse, *Chem. Soc. Rev.* 2012, **41**, 7335.
7 J.-F. Lemonnier, S. Duval, S. Floquet, E. Cadot, *Isr. J. Chem.* 2011, **51**, 290.
8 J. M. Gretarsdóttir, S. Bobersky, N. Metzler-Nolte, S. G. Suman, *J. Inorg. Biochem*. 2016, **160**, 166.
9 S. G. Suman, J. M. Gretarsdottir, P. E. Penwell, J. P. Gunnarsson, S. Frostason, S. Jonsdottir, K. K. Damodaran and A. Hirschon, *Inorg. Chem.* 2020, **59**, 7644.
10 J. M. Gretarsdottir, S. Jonsdottir, W. Lewis, T. W. Hambley and S. G. Suman, *Inorg. Chem*. 2020, **59**, 18190.
11 S. G. Suman, J. M. Gretarsdottir, T. Snaebjornsson, G. R. Runarsdottir, P. E. Penwell, S. Brill and C. Green, *J. Biol. Inorg. Chem*. 2014, **19**, S760.
12 A. Fuior, A. Hijazi, O. Garbuz, V. Bulimaga, L. Zosim, D. Cebotari, M. Haouas, I. Toderas, A. Gulea and S. Floquet, *J. Inorg. Biochem*. 2022, **226**, 111627.
13 S. Mckenzie-Nickson, A. I. Bush and K. J. Barnham, *Curr. Top. Med. Chem*. 2016, **16**, 3058.
14 M. S. More, P. G. Joshi, Y. K. Mishra and P. K. Khanna, *Mater. Today Chem*. 2019, **14**, 100195.
15 A. M. Merlot, D. S. Kalinowski and D. R. Richardson, *Antioxid. Redox Signal.* 2013, **18**, 973.
16 Y. Yu, D. S. Kalinowski, Z. Kovacevic, A. R. Siafakas, P. J. Jansson, C. Stefani, D. B. Lovejoy, P. C. Sharpe, P. V. Bernhardt and D. R. Richardson, *J. Med. Chem*. 2009, **52**, 5271.
17 A. Matesanz, J. M. Herrero and A. G. Quiroga, *Curr. Top. Med. Chem*. 2021, **21**, 59.
18 H. Beraldo and D. Gambino, *Mini-Rev. Med. Chem.* 2004, **4**, 31.
19 D. S. Kalinowski, P. Quach and D. R. Richardson, *Future Med. Chem. 2009*, **1**, 1143.
20 A. K. Moharana, R. N. Dash and B. B. Subudhi, *Mini-Rev. Med. Chem*. 2021, **20**, 2135.
21 B. Shakya and P. N. Yadav, *Mini-Rev. Med. Chem.* 2020, **20**, 638.
22 J. de O. Carneiro Brum, T. C. Costa Franca and J. D. Figueroa Villar, *Mini-Rev. Med. Chem.* 2020, **20**, 342.
23 L. R. Pessoa de Siqueira, P. A. Teixeira de Moraes Gomes, L. P. de Lima Ferreira, M. J. Barreto de Melo Rego and A. C. Lima Leite, *J. Med. Chem*. 2019, **170**, 237.
24 K. Haldys and R. Latajka, *Medchemcomm* 2019, **10**, 378.
25 C. B. Scarim, D. H. Jornada, M. G. M. Machado, C. M. R. Ferreira, J. L. dos Santos, M. C. Chung, *Eur. J. Med. Chem*. 2019, **162**, 378.
26 A. C. Lima Leite, J. W. Pontes Espindola, M. V. de Oliveira Cardoso, G. B. de Oliveira Filho. *Curr. Med. Chem*. 2019, **26**, 4323.
27 K. L. Summers, *Mini-Rev. Med. Chem*. 2019, **19**, 569.
28 P. Heffeter, V. F. S. Pape, E. A. Enyedy, B. K. Keppler, G. Szakacs and C. R. Kowol, *Antioxid. Redox Signal*. 2019, **30**, 1062.
29 J.-X. Liang, H.-J. Zhong, G. Yang, K. Vellaisamy, D.-L. Ma and C.-H. Leung, *J. Inorg. Biochem*. 2017, **177**, 276.
30 S. Eglence-Bakir, O. Sacan, M. Sahin, R. Yanardag and B. Ulkuseven, *J. Mol. Struct*. 2019, **1194**, 35.
31 V. Vrdoljak, I. Đilović, M. Rubčić, S. Kraljević Pavelić, M. Kralj, D. Matković-Calogović, I. Piantanida, P. Novak, A. Rožman and M. Cindrić, *Eur. J. Med. Chem*. 2010, **45**, 38.
32 S. Celen, S. Eglence-Bakir, M. Sahin, I. Deniz, H. Celik and I. Kizilcikli, *J. Coord. Chem*. 2019, **72**, 1747.
33 J. Pisk, B. Prugovecki, D. Matkovic-Calogovic, R. Poli, D. Agustin, V. Vrdoljak, *Polyhedron*, 2012, **33**, 441.
34 A. Fuior, D. Cebotari, M. Haouas, J. Marrot, G. Minguez Espallargas, V. Guérineau, D. Touboul, R. V. Rusnac, A. Gulea and S. Floquet, *ACS Omega*, 2022, **7**, 16547.
35 G. M. Sheldrick, Vol. SADABS program for scaling and correction of area detector data 1997.
36 G. M. Sheldrick, *Acta Cryst C*, 2015, **71**, 3.
37 C. B. Hübschle, G. M. Sheldrick and B. Dittrich, *J Appl Crystallogr*, 2011, **44**, 1281.
38 H. R. Darabi, S. Rastgar, K. Aghapoor and F. Mohsenzadeh, *Monatsh. Chem.*, 2018, **149**, 1121.
39 D. Nakatake, Y. Yokote, Y. Matsushima, R. Yazaki and T. Ohshima, *Green Chem.*, 2016, **18**, 1524.
40 K. Murai, S. Fukushima, A. Nakamura, M. Shimura and H. Fujioka, *Tetrahedron*, 2011, **67**, 4862.
41 T. K. Venkatachalam, P. V. Bernhardt, G. K. Pierens, D. C. Reutens, *J. Chem. Crystallogr.,* 2017, **47**, 30.
42 J. Pisk, B. Prugovecki, D. Matkovic-Calogovic, R. Poli, D. Agustin and V. Vrdoljak, *Polyhedron*, 2012, **33**, 441.
43 V. Vrdoljak, D. Milic, M. Cindric, D. Matkovic-Calogovic, J. Pisk, M. Markovic and P. Novak, *Z. Anorg. Allg. Chem*., 2009, **635**, 1242.
44 V. Vrdoljak, J. Pisk, B. Prugovecki and D. Matkovic-Calogovic, *Inorg. Chim. Acta*, 2009, **362**, 4059.
45 V. Vrdoljak, D. Milic, M. Cindric, D. Matkovic-Calogovic and D. Cincic, *Polyhedron*, 2007, **26**, 3363.
46 S. Floquet, N. Guillou, P. Negrier, E. Riviere, M.-L. Boillot, *New J. Chem.* 2006, **30**, 1621.
47 S. Floquet, S. Brun, J.-F. Lemonnier, M. Henry, M.-A. Delsuc, Y. Prigent, E. Cadot, F. Taulelle, *J. Am. Chem. Soc.* 2009, **131**, 17254.